JACS
JOURNAL OF THE AMERICAN CHEMICAL SOCIETY

COMMUNICATION

pubs.acs.org/JACS

High Proton Conduction in a Chiral Ferromagnetic Metal−Organic Quartz-like Framework

Emilio Pardo,[†,⊥] Cyrille Train,*[,‡] Geoffrey Gontard,[†] Kamal Boubekeur,[†] Oscar Fabelo,[§] Hongbo Liu,[∥] Brahim Dkhil,[∥] Francesc Lloret,[⊥] Kosuke Nakagawa,[#] Hiroko Tokoro,[#] Shin-ichi Ohkoshi,[#] and Michel Verdaguer*[,†]

[†]Institut Parisien de Chimie Moléculaire, Université Pierre et Marie Curie-Paris 6, UMR CNRS 7201, 75252 Paris cedex 05, France

[‡]Laboratoire National des Champs Magnétiques Intenses, UPR CNRS 3228, Université Joseph Fourier, B.P. 166, 38042 Grenoble cedex 9, France

[§]Institut Laue Langevin, BP 156, F-38042 Grenoble cedex 9, France

[∥]Laboratoire Structures, Propriétés et Modélisation des Solides, UMR CNRS 8580, Ecole Centrale Paris, 92295 Châtenay-Malabry cedex, France

[⊥]Departament de Química Inorgànica, Instituto de Ciencia Molecular (ICMOL), Universitat de València, 46980 Paterna, València, Spain

[#]Department of Chemistry, School of Science, The University of Tokyo, 7-3-1 Hongo, Bunkyo-ku, Tokyo 113-0033, Japan

Supporting Information

ABSTRACT: A complex-as-ligand strategy to get a multifunctional molecular material led to a metal−organic framework with the formula $(NH_4)_4[MnCr_2(ox)_6]\cdot 4H_2O$. Single-crystal X-ray diffraction revealed that the anionic bimetallic coordination network adopts a chiral three-dimensional quartz-like architecture. It hosts ammonium cations and water molecules in functionalized channels. In addition to ferromagnetic ordering below $T_C = 3.0$ K related to the host network, the material exhibits a very high proton conductivity of 1.1×10^{-3} S cm^{-1} at room temperature due to the guest molecules.

The design and synthesis of multifunctional magnetic molecular materials (M_4)[1] showing different and peculiar functionalities in addition to and/or interacting with the magnetic properties (i.e., photomagnetism,[1a] nonlinear magnetooptics,[1b] gas adsorption,[1c] magnetochiral dichroism,[1d] etc.) represent an active research area for chemists, physicists, and materials scientists. Two- or three-dimensional (2D or 3D) coordination compounds, sometimes named metal−organic frameworks (MOFs),[2] are appropriate candidates for the synthesis of such new M_4. A wide variety of architectures can indeed be obtained in a rational and versatile way to combine the intrinsic properties of the host (magnetic, optical, etc.) with specific ones due to the selected guest molecules. New knowledge and potential technological applications in very different fields such as molecular electronics and spintronics,[3] gas storage and transport, molecular sensing, and catalysis[4] can be expected through exploitation of the combination and/or interaction of two (or more) properties existing in M_4.

In the search for additional physical properties, solid-state proton conductivity is nowadays challenging for both potential fuel cell applications[6] and a better understanding in the field of transport dynamics.[5,6] However, proton conductivity requires proton carriers such as H_3O^+, NH_4^+, or H^+ belonging to acid groups or to networks of hydrogen bonds,[7] and only a few works related to proton conductivity of MOFs have been reported.[7]

Here we present an oxalate-based bimetallic 3D chiral anionic network with the formula $(NH_4)_4[MnCr_2(ox)_6]\cdot 4H_2O$ (**1**), the structure of which is reminiscent of β-quartz.[8] A long-range ferromagnetic ordering at low temperature is provided by the host anionic network, whereas the counterions and the guest molecules, which are located around the oxalate network and in the channels of the structure, give rise to high room-temperature protonic conductivity.

Compound **1** was obtained as large purple parallelepipeds from the reaction of ammonium tris(oxalato)chromate(III) and manganese(II) chloride in water and slow diffusion of ethanol. The crystal structure of **1** was solved by single-crystal X-ray diffraction. **1** crystallizes in the chiral $P6_522$ space group.

In **1**, each chromium ion is bound to three bidentate oxalate ligands to form a distorted D_3 unit and a six-coordinate distorted oxygen octahedron [Cr−O bond distances in the range 1.963(3)−1.987(3) Å]. Each chromium is located in a general position, and the tris(oxalato)chromate(III) units form a helix around the 6_5 axis (Figure 1). One of the oxalate ligands is directed toward crystallization water molecules along the helical axis. The other two oxalate ligands bridge chromium(III) to manganese(II) ions in a bis-bidentate way. In turn, each manganese(II) ion is located at the intersection of three C_2 axes and linked to four chromium(III) by oxalate bridges (Figure 1). The coordination number of the manganese atom is therefore 8, and the compound exhibits a 2:1 Cr:Mn stoichiometry. The geometry around the manganese atoms can be described as a bicapped triangular prism involving eight oxygen atoms from four bidentate oxalate groups, with four short [2.223(3)−2.234(3) Å] Mn−O distances, two intermediate [2.394(3) Å] Mn−O distances within the prism, and two long [2.528(4) Å]

Received: July 25, 2011
Published: September 13, 2011

dx.doi.org/10.1021/ja206917z | J. Am. Chem. Soc. 2011, 133, 15328–15331

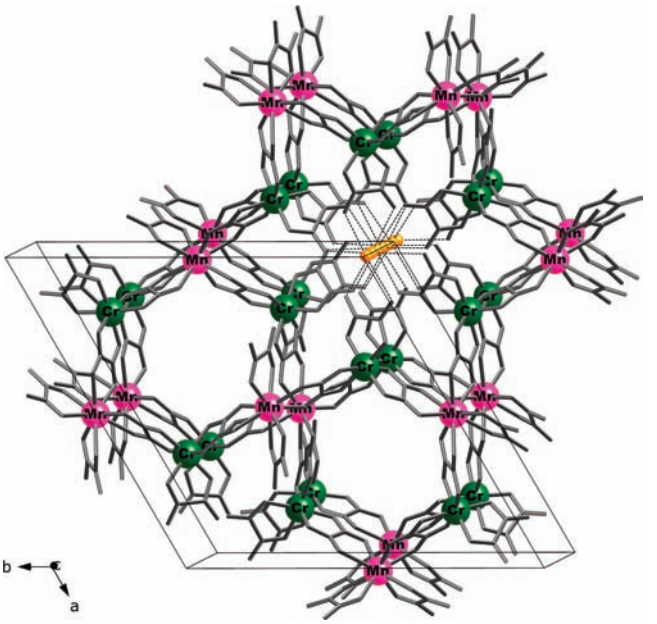

Figure 1. Perspective view of a fragment of the 3D anionic network of **1** with the metal atoms labeled. Metal and ligand atoms are represented by balls (Cr, green; Mn, purple) and sticks, respectively. Guest water molecules located in the A channels are shown in orange. Hydrogen atoms have been omitted for clarity.

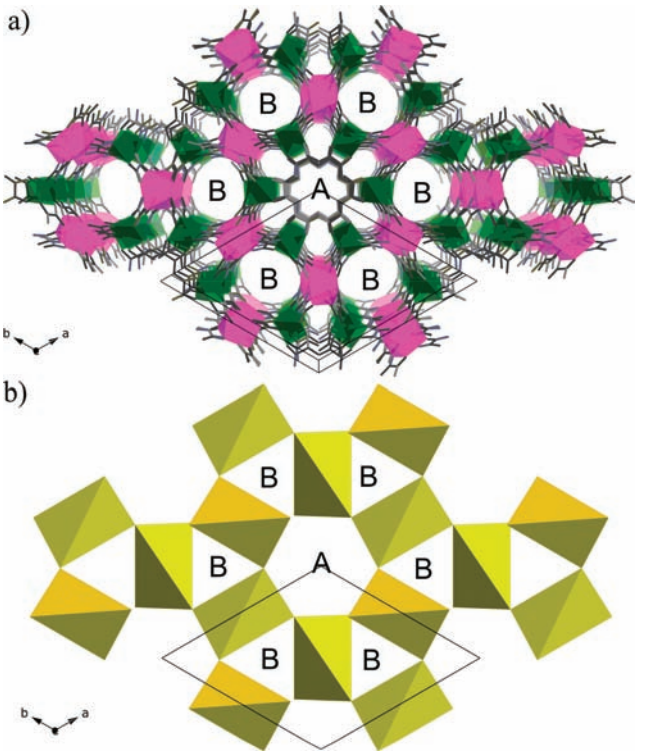

Figure 2. Views of the crystal structure along the *c* axis of the bimetallic network, (a) emphasizing the environment of Cr(III) and Mn(II) (pink and green polyhedra, respectively) and the presence of two types of channels (A along the 6_5 axis and B along the 3 axis) and (b) underlining the quartz-like organization of the $MnCr_4$ tetrahedra, shown in yellow-brown.

Mn−O distances for the caps. $[M(ox)_4]^{n-}$ moieties are well-known for heavy-metal ions from the s, p, and f blocks but are scarce for transition-metal ions.[9] The coordination mode of the chromium(III) metalloligand has been observed previously only in a handful of compounds.[10]

In a networking view,[11] the $[Cr^{III}(ox)_3]^{3-}$ moieties act as 2-connectors and the $[Mn^{II}(ox)_4]^{6-}$ moieties as 4-connectors (Figure 1). The distances between bridged chromium(III) and manganese(II) ions are in the range 5.516(1)−5.619(1) Å. The connectivities of both metal ions give birth to a 3D oxalate-based anionic network, $[Mn^{II}Cr^{III}_2(ox)_6]^{4-}$, with a $(6^4\cdot8^2)$ net topology (Figure 2a).[11] It is rewarding to examine how the $MnCr_4$ units build the network. Each $MnCr_4$ unit is a tetrahedron that is heavily flattened along the *c* axis [33.25(1)° dihedral angle]. The $MnCr_4$ tetrahedra share vertices and build a helical arrangement along the *c* axis that leads to the 3D anionic framework (Figure 2b). The network of **1** (space group $P6_522$) then appears as a molecular analogue of *β*-quartz (space group $P6_422$) with a flattened helical arrangement along the *c* axis. In contrast to *β*-quartz, the MOF contains a chiral element, namely, the helical $[Cr(ox)_3]^{3-}$ moieties. Because of the absence of improper symmetry operations in the observed space group, all of these metal centers exhibit the same absolute configuration (*Λ* in the present enantiomer **1**) and there is only one type of helix (*M* in **1**). Following a second-order spontaneous resolution process, the resulting network is indeed enantiopure.[12] The length of the metalloligand bridging the Mn(II) induces a distance between the manganese centers of 10.079(1) Å. This can be compared with the distance of 3.09 Å between the oxo-bridged Si(IV) in *β*-quartz. Accordingly, there is a strong increase in the diameters of the channels in **1**, which reach 5.23 Å for the A channels and 7.52 Å for the B channels (Figure 2).

The A channels are functionalized by the terminal oxalate ligand of the $[Cr(ox)_3]^{3-}$ moieties. This favors the insertion of guest water molecules at the center of the channel [half occupancy O(3w) and O(4w); Figure 1 and Figure S1 in the Supporting Information], which form 1D ribbons running along the channel. The B channels also welcome water molecules, which were revealed by residual electronic density but were too highly disordered to be properly attributed. The corresponding void measures 585 Å^3, which represents 11% of the unit cell volume [V = 5232.0(15) Å^3]. Two other crystallization water molecules are found nearby, outside the A and B channels [half occupancy O(1w) and quarter occupancy O(2w)]. Ammonium cations located close to the helices (unit occupancy for N1, N2, N3) compensate for the four negative charges of the repeating unit of the bimetallic coordination network.

Disorder was observed on some of these molecules, but a striking feature is the formation, around the 6_5 A channels, of a well-defined helical chain of ammonium cations [N···N = 2.839(7)−2.892(6) Å] exhibiting hydrogen-bonding interactions with the oxygen atoms of the terminal oxalates [N···O = 2.795(6)−2.960(8) Å], which in turn are connected to the central guest water molecules of the A channel [O(11,12)···O(3,4w) = 2.745(13)−2.888(16) Å]. Finally, O(1w) and O(2w) also take part in the hydrogen-bonding network [O(1,2w)···O(5,9,11) = 2.795(15)−2.972(15) Å; O(1,2w)···N2 = 2.780(28)−2.924(14) Å].

In order to determine the amount of water molecules in **1**, thermogravimetric analysis (TGA) under a dry N_2 atmosphere was performed. It showed a slow mass loss from room temperature to ∼140 °C followed by a plateau under further heating up

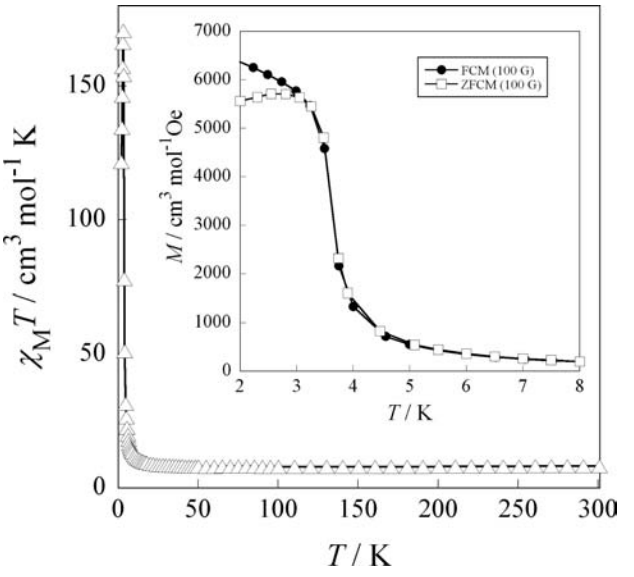

Figure 3. Temperature dependence of $\chi_M T$ of **1** (△) in an applied magnetic field of 1 T ($T \geq 50$ K) or 100 G ($T < 50$ K). The inset shows the field-cooled magnetization (FCM, measured upon cooling within the field) (●) and the zero-field-cooled magnetization (ZFCM, measured after cooling in zero field and then warming within the field) (□). The solid lines are eye-guides only.

to 265 °C, where decomposition starts (Figure S2). The percentage of the mass loss was ~9%, a value that corresponds to four water molecules per formula unit. This loss of mass in **1** is then attributed to the release of all the crystallization water molecules: 2.5 water molecules corresponding to O(1w)−O(4w) as identified by single-crystal X-ray diffraction and ~1.5 water molecules corresponding to the disordered residual electronic density found in the B channels (not represented).

These structural features give rise to the following physicochemical properties. The thermal variation of $\chi_M T$ of **1**, where χ_M is the molar magnetic susceptibility per $MnCr_2$ unit and T is the absolute temperature, is shown in Figure 3. The $\chi_M T$ value of 8.20 $cm^3\ mol^{-1}\ K$ at room temperature is close to that expected for the sum of one octahedral high-spin Mn^{II} ion ($S_{Mn} = {}^5/_2$; $\chi_M T$ = 4.37 $cm^3\ mol^{-1}\ K$ with $g_{Mn} = 2.0$) and two octahedral Cr^{III} ions ($S_{Cr} = {}^3/_2$; $\chi_M T$ = 1.87 $cm^3\ mol^{-1}\ K$ with $g_{Cr} = 2.0$). As T decreases, $\chi_M T$ rises continuously until it reaches a maximum value of 170 $cm^3\ mol^{-1}\ K$ at ~3.0 K. This behavior is consistent with ferromagnetic coupling between the high-spin Mn^{II} and the Cr^{III} ions through the oxalate bridge.

A paramagnetic-to-ferromagnetic phase transition at T_C = 3.0 K is revealed by (*i*) the temperature dependence of the field-cooled magnetization (FCM) and the zero-field-cooled magnetization (ZFCM) (Figure 3 inset) and (*ii*) the ac magnetic properties (Figure S3 inset). This ferromagnetic ordering has been found previously in other oxalato-based 2D and 3D bimetallic compounds with higher Curie temperatures ($T_C \approx 6.0$ K[1d] or 5.5 K[7h]). We suggest that the smaller T_C in **1** may be attributed to the smaller spin density present on the neighboring oxygen atoms of manganese in **1**, which is due to the increase in the number of neighbors from 6 to 8, to the larger oxalate oxygen−manganese distances, and to the very low symmetry of the highly distorted octacoordinate environment of the Mn^{II} ions.

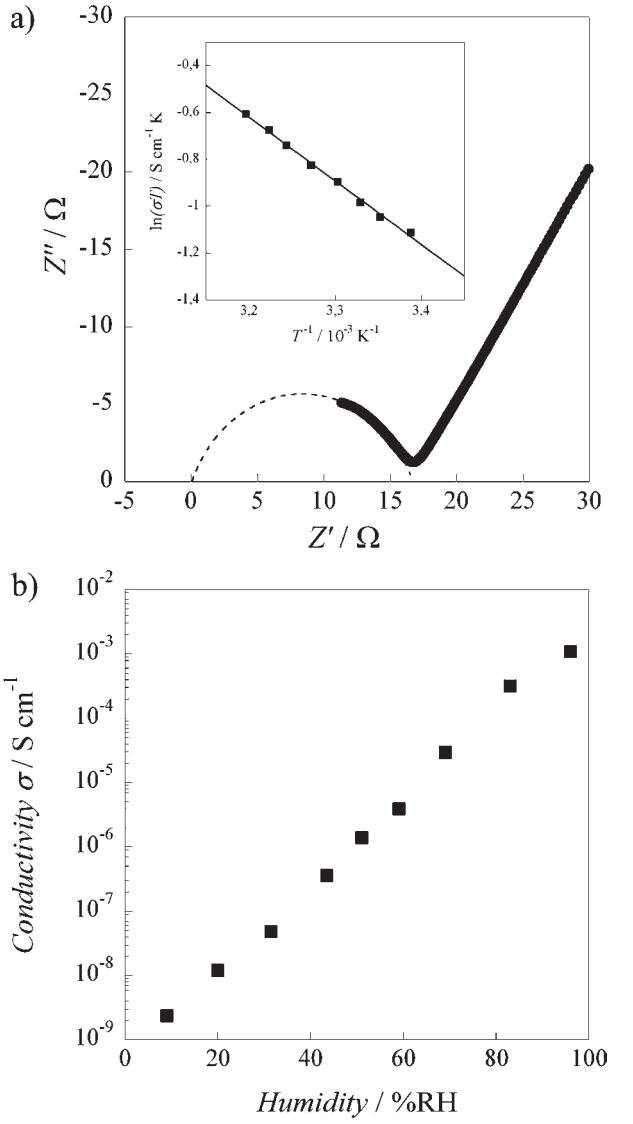

Figure 4. (a) Z'-vs-Z'' plot of complex-plane impedance for **1** at 295 K and 96% RH. The inset shows an Arrhenius-type plot of the conductivity of **1** at various temperatures. (b) Relative humidity dependence of the conductivity (σ) for **1** at 295 K.

Figure 4a shows the real (Z') and imaginary (Z'') parts of the complex-plane impedance data for **1**. Cole−Cole circular arc fitting gave a conductivity (σ) value of 1.1×10^{-3} S cm^{-1} at 295 K and 96% relative humidity (RH), which increased to 1.7×10^{-3} S cm^{-1} at 313 K. The plot of $\ln(\sigma T)$ versus T^{-1} is linear (Figure 4a inset), indicating that the activation energy (E_a) of the ionic conductivity is 0.23 eV. With increasing humidity, the σ value increased by 5 orders of magnitude, from 2.4×10^{-9} S cm^{-1} at 9% RH to 1.1×10^{-3} S cm^{-1} at 96% RH (Figure 4b). These two features confirm that proton conductivity is responsible for the high conductivity of **1** and should occur through a Grotthus mechanism.[13]

The σ value of 2.3×10^{-3} S cm^{-1} at 91.5% RH allows **1** to be classified as a superionic conductor ($\sigma > 10^{-4}$ S cm^{-1}).[13] The value of the proton conductivity of **1** is very high and similar to the values reported for the very few other examples of MOFs showing high proton conductivity.[13] It is only slightly lower than that of Nafion, a reference compound in the field.[14] It would be

dx.doi.org/10.1021/ja206917z |*J. Am. Chem. Soc.* 2011, 133, 15328–15331

unwise at the present stage to propose a definitive conduction mechanism. Nevertheless, the hydrogen-bonding continuum implying peripheral guests and central water molecules of the functionalized 6_5 A channels (Figure S1) is an attractive candidate as a pathway for the proton conduction triggered by humidity.

In conclusion, we have synthesized a new MOF combining chirality, ferromagnetism, and very high proton conduction. Our rational approach was based (*i*) for the chirality, on the D_3 symmetry of the $[Cr(ox)_3]^{3-}$ precursor; (*ii*) for the magnetic properties, on the well-known ferromagnetic interaction between Cr(III) and Mn(II) ions through oxalate bridges;[10] and (*iii*) for the proton conductivity, on the introduction of proton carriers such as NH_4^+ cations close to water in functionalized channels thanks to a synthesis in an aqueous medium. We are now exploring the other remarkable properties of the compound, including the second-order spontaneous resolution process that appears in the synthesis.

■ ASSOCIATED CONTENT

Supporting Information. Experimental preparation; analytical and spectroscopic characterization of **1**; additional figures showing structural details, TGA data, and magnetization data; and X-ray data in CIF format. This material is available free of charge via the Internet at http://pubs.acs.org.

■ AUTHOR INFORMATION

Corresponding Author
cyrille.train@lncmi.cnrs.fr; michel.verdaguer@upmc.fr

■ ACKNOWLEDGMENT

This work was supported by the Centre National de la Recherche Scientifique (CNRS, France), the Ministère de l'Enseignement Supérieur et de la Recherche (MESR, France), the Agence Nationale de la Recherche (ANR, France; Project ANR-08-JCJC-0113-01), the MICINN (Spain) (Projects CTQ2010-15364 and CSD2007-00010). E.P. and C.T. acknowledge the MEC and the Japan Society for the Promotion of Science (JSPS) for their respective postdoctoral grants. The authors thank Prof. J. Elguero (CSIC, Spain) for fruitful discussions and continuous interest in this work.

■ REFERENCES

(1) (a) Sato, O. *Acc. Chem. Res.* **2003**, *36*, 9692. (b) Nuida, T.; Matsuda, T.; Tokoro, H.; Sakurai, S.; Hashimoto, K.; Ohkoshi, S. *J. Am. Chem. Soc.* **2005**, *127*, 11604. (c) Long, J. R.; Yaghi, O. M. *Chem. Soc. Rev.* **2009**, *38*, 1213. (d) Train, C.; Gheorghe, R.; Krstic, V.; Chamoreau, L. M.; Ovanesyan, N. S.; Rikken, G. L. J. A.; Gruselle, M.; Verdaguer, M. *Nat. Mater.* **2008**, *9*, 729. (e) Ohkoshi, S.; Arai, K.; Sato, Y.; Hashimoto, K. *Nat. Mater.* **2004**, *3*, 857. (f) Train, C.; Gruselle, M.; Verdaguer, M. *Chem. Soc. Rev.* **2011**, *40*, 3297.

(2) (a) Batten, S. R.; Robson, R. *Angew. Chem., Int. Ed.* **1998**, *37*, 1460. (b) Janiak, C. *Dalton Trans.* **2003**, 2781. (c) Maspoch, D.; Ruiz-Molina, D.; Veciana, J. *Chem. Soc. Rev.* **2007**, *36*, 770. (d) Maspoch, D.; Ruiz-Molina, D.; Wurst, K.; Domingo, N.; Cavallini, M.; Biscarini, F.; Tejada, J.; Rovira, C.; Veciana, J. *Nat. Mater.* **2003**, *2*, 190. (e) Dechambenoit, P.; Long, J. R. *Chem. Soc. Rev.* **2011**, *40*, 3249.

(3) (a) Turnbull, M. M.; Sugimoto, T.; Thompson, L. K.; *Molecule-Based Magnetic Materials*; American Chemical Society: Washington, DC, 1996. (b) Sanvito, S. *Chem. Soc. Rev.* **2011**, *40*, 3336.

(4) (a) Yaghi, O. M.; O'Keeffe, M.; Eddaoudi, M.; Chae, H. K.; Kim, J.; Ockwig, N. W. *Nature* **2003**, *423*, 705. (b) Kitagawa, S.; Kitaura, R.; Noro, S.-I. *Angew. Chem., Int. Ed.* **2004**, *43*, 2334. (c) Férey, G. *Chem. Soc. Rev.* **2008**, *37*, 191.

(5) (a) Wood, B. C.; Marzari, N. *Phys. Rev. B* **2007**, *76*, No. 134301. (b) Yu, R.; Jonghe, L. C. D. *J. Phys. Chem. C* **2007**, *111*, 11003.

(6) (a) Kreuer, K. D.; Paddison, S. J.; Spohr, E.; Schuster, M. *Chem. Rev.* **2004**, *104*, 4637. (b) Steele, B. C.; Heinzel, A. *Nature* **2001**, *414*, 345.

(7) (a) Kitagawa, H.; Nagao, Y.; Fujishima, M.; Ikeda, R.; Kanda, S. *Inorg. Chem. Commun.* **2003**, *6*, 346. (b) Nagao, Y.; Kubo, T.; Nakasuji, K.; Ikeda, R.; Kojima, T.; Kitagawa, H. *Synth. Met.* **2005**, *154*, 89. (c) Fujishima, M.; Enyo, M.; Kanda, S.; Ikeda, R.; Kitagawa, H. *Chem. Lett.* **2006**, *35*, 546. (d) Yamada, T.; Sadakiyo, M.; Kitagawa, H. *J. Am. Chem. Soc.* **2009**, *131*, 3144. (e) Sadakiyo, M.; Yamada, T.; Kitagawa, H. *J. Am. Chem. Soc.* **2009**, *131*, 9906. (f) Bureekaew, S.; Horike, S.; Higuchi, M.; Mizuno, M.; Kawamura, T.; Tanaka, D.; Yanai, N.; Kitagawa, S. *Nat. Mater.* **2009**, *8*, 831. (g) Hurd, J. A.; Vaidhyanathan, R.; Thangadurai, V.; Ratcliffe, C. I.; Moudrakovski, I. L.; Shimizu, G. K. H. *Nat. Chem.* **2009**, *1*, 705. (h) Ōkawa, H.; Shigematsu, A.; Sadakiyo, M.; Miyagawa, T.; Yoneda, K.; Ohba, M.; Kitagawa, H. *J. Am. Chem. Soc.* **2009**, *131*, 13516. (i) Ohkoshi, S. M.; Nakagawa, K.; Tomono, K.; Imoto, K.; Tsunobuchi, Y.; Tokoro, H. *J. Am. Chem. Soc.* **2010**, *132*, 6620.

(8) (a) Wu, Y.; Li, D.; Fu, F.; Tang, L.; Wang, J.; Yang, X. G. *J. Coord. Chem.* **2009**, *62*, 2665. (b) Sun, J.; Weng, L.; Zhou, Y.; Chen, J.; Chen, Z.; Liu, Z.; Zhao, D. *Angew. Chem., Int. Ed.* **2002**, *41*, 4471.

(9) (a) Rochon, F. D.; Melanson, R.; Andruh, M. *Inorg. Chem.* **1996**, *35*, 6086. (b) Armentano, D.; De Munno, G.; Mastropietro, T. F.; Julve, M.; Lloret, F. *Chem. Commun.* **2004**, 1160. (c) Cotton, F. A.; Diebold, M. P.; Roth, W. J. *Inorg. Chem.* **1987**, *26*, 288.

(10) (a) Ohba, M.; Tamaki, H.; Matsumoto, N.; Okawa, H. *Inorg. Chem.* **1993**, *32*, 5385. (b) Pardo, E.; Train, C.; Lescouëzec, R.; Boubekeur, K.; Ruiz, E.; Lloret, F.; Verdaguer, M. *Dalton Trans.* **2010**, *39*, 4951. (c) Clemente-León, M.; Coronado, E.; Dias, J. C.; Soriano-Portillo, A.; Willet, R. D. *Inorg. Chem.* **2008**, *47*, 6458.

(11) Wells, A. F.; *Structural Inorganic Chemistry*, 4th ed.; Clarendon Press: Oxford, U.K., 1975.

(12) Tong, X.-L.; Hu, T.-L.; Zhao, J.-P.; Wang, Y.-K.; Zhang, H.; Bu, X.-H. *Chem. Commun.* **2010**, *46*, 8543.

(13) (a) Colomban, P.; Novak, A. *J. Mol. Struct.* **1988**, *177*, 277. (b) Colomban, P. *Proton Conductors: Solids, Membranes and Gels—Materials and Devices*; Cambridge University Press: Cambridge, U.K., 1992.

(14) (a) Slade, R. C. T.; Hardwick, A.; Dickens, P. G. *Solid State Ionics* **1983**, *9*, 1093. (b) Alberti, G.; Casciola, M. *Solid State Ionics* **2001**, *145*, 3.